J. Meas. Sci. Instrum., 2023, 14(3): 315-323
DOI: 10.3969/j.issn.1674-8042.2023.03.008
http://xuebao.nuc.edu.cn
jmsi@nuc.edu.cn

Dual-PMSM speed synchronization control based on unified prediction model

MIAO Zhongcui[1,2], HE Yangyang[1], LI Haiyuan[1], WANG Yunkun[1]

(1. *School of Automation and Electrical Engineering, Lanzhou Jiaotong University, Lanzhou 730070, China*;
2. *Key Laboratory of Opto-Technology and Intelligent Control of Ministry Education, Lanzhou Jiaotong University, Lanzhou 730070, China*)

Abstract: In a dual-motor control system, load disturbance and parameter vatiation as well as acceleration/deceleration operation will lead to instability of the system, which makes synchronization error increase. To solve the above problems, a speed synchronization control system based on the unified predictive model of a dual-motor is designed. First of all, a unified dual-motor model is established on the basis of the traditional dual-motor cross-coupled control structure, and a piecewise value function is constructed to adjust tracking error and synchronization error more accurately. Secondly, to improve the dynamic performance and robustness of the system, a proportional-integral + fractional order sliding mode control (PI + FOSMC) compound synchronization controller is designed. Finally, the simulation is carried out on two permanent magnet synchronous motors (PMSMs). The result shows that the dual-motor unified prediction system has strong dynamic performance and robustness, and can improve synchronization accuracy.

Key words: permanent magnet synchronous motor (PMSM); dual-motor control; cross-coupled control; unified prediction model; speed synchronization controller; synchronization accuracy

0 Introduction

Permanent magnet synchronous motor (PMSM) is widely used owing to its simple structure, high efficiency and high power density. With the change of industrial production demand, high-power drive systems are needed in many applications, such as cranes, paper machines, machine tools and some electric vehicles. To meet the requirements of output power, dual-motor or multi-motor drive is needed. For multi-motor control system, the performance of speed synchronization directly affects the system reliability and industrial production efficiency[1-3]. Therefore, it is very important to study the dual-motor synchronous control system to improve the control performance.

Using a dual-motor control system to drive the load, the speed of the two motors needs to be synchronized, but the disturbances in an operating environment, the change of motor parameters and the acceleration and deceleration operations of the system will lead to large synchronization error and torque ripple between the two motors, which may damage the equipment structure and even affect the production safety[4-5]. Generally, the dual motor drive system is driven by gears, but the load distribution is uneven in this way, which causes the speed difference between the motors. In addition, the influence of external factors reduces the stability and synchronization accuracy of the system. Therefore, it is necessary to improve robustness and synchronization accuracy of the dual-motor control system, so as to improve the production efficiency and ensure production safety[6].

Model predictive control is widely used in motor control because of its fast dynamic response, strong robustness and high steady-state accuracy, which can fully consider the nonlinear characteristics of the system and the constraints of variables, so that it is easier to achieve multi-objective control[7-8]. Value function is an important part of model predictive control, and value directly determines the final selection of the optimal voltage vector, therefore it is very important to select the appropriate value

Received date: 2022-11-14
Foundation items: National Natural Science Foundation of China (No. 51867012)
Corresponding author: HE Yangyang (1054997624 @qq.com)

function for model predictive control[9-10]. In many literatures, by improving the value function, the control performance of the system is improved. Tu et al.[11] proposed a fuzzy algorithm to adjust the weight factor in the objective function online, which effectively improves the control performance of the motor. Wang et al.[12] introduced synchronization error term into value function to improve speed synchronization accuracy. Shi et al.[13] established a quadratic value function and obtained good control performance. However, the value function has many constraints, and the weight coefficient matrix needs to be calculated offline.

Improving the anti-interference performance and dynamic performance of the system can improve the synchronization accuracy of the two motors. At present, the research of dual motor control system mainly focuses on improving control structure and control algorithm. The control structure adopts master-slave control, parallel control, deviation coupling control, cross coupling control, virtual spindle control and so on[14]. Among them, the structure of cross coupling control is simple, the synchronization error of two motors can be compensated by synchronization controller, and the synchronization accuracy is high, which is suitable for double motor synchronization control[6,14]. The improvement of the control algorithm aims to improve the performance of the controller. In the traditional dual-motor synchronous control system, the synchronous controller mostly adopts proportional-integral controller (PI), which is simple, fast, highly steady-state precisce, but poorly robust[15]. Sliding mode control is a nonlinear control method, which is independent of system parameters and has strong robustness, so that the system is not easy to be affected by the disturbance in the operation process, physical implementation is simple, and the control performance of the motor can be effectively improved[16]. Fractional calculus inherits the advantages of integral calculus, and the degree of freedom of adjustable parameters is increased. Reasonable choice of calculus order can increase the flexibility of control system. Combining fractional calculus and sliding mode control can not only speed up the response speed of the sliding mode controller, but enhance the robustness of the control system. Nan et al.[17-19] used fractional-order sliding mode control is used for single-motor control and has good performance. To reduce the influence of load disturbance, suppress the chattering caused by sliding mode control, Gao et al.[20-21] established a load observer to estimate the disturbance in the system and achieved a good control effect.

In this study, the dual permanent magnet synchronous motor (PMSM) control system is taken as the object, aiming at the problems of poor dynamic performance, poor robustness and low synchronization accuracy, a dual-motor synchronous control system based on unified predictive model is established to improve the synchronous controller. Firstly, we establish a dual-motor unified prediction model, and piecewise value function is constructed. Then, to improve the dynamic performance and robustness of the system, a compound synchronous controller is designed, with the advantages of fractional order sliding mode control (FOSMC) and PI control. In addition, a sliding mode disturbance observer is designed, and the its value is input into FOSMC. Finally, the simulation is carried out on Matlab.

1 Establishment of system model

1.1 Mathematical model of PMSM

In the d-q coordinate system, the mathematical model of the ith PMSM is

$$\begin{bmatrix} \dfrac{\mathrm{d}i_{di}}{\mathrm{d}t} \\ \dfrac{\mathrm{d}i_{qi}}{\mathrm{d}t} \end{bmatrix} = \begin{bmatrix} -\dfrac{R_i}{L_i} & \omega_{ei} \\ -\omega_{ei} & -\dfrac{R_i}{L_i} \end{bmatrix} \begin{bmatrix} i_{di} \\ i_{qi} \end{bmatrix} + \begin{bmatrix} \dfrac{1}{L_i} & 0 \\ 0 & \dfrac{1}{L_i} \end{bmatrix} \begin{bmatrix} u_{di} \\ u_{qi} \end{bmatrix} - \begin{bmatrix} 0 \\ \dfrac{\psi_{fi}\omega_{ei}}{L_i} \end{bmatrix}, \tag{1}$$

where i stands for the ith motor ($i=1,2,$); u_{di} and u_{qi} are the voltages of d-q axis, respectively; i_{di} and i_{qi} are the currents of d-q axis, respectively; ω_{ei} is the electric angular velocity of the PMSM; p is the number of state pole pairs; $\omega_{ei}=p_i\omega_{mi}$, and ω_{mi} is the mechanical angular velocity of the PMSM; ψ_{fi}, R_i and L_i are the permanent magnet flux linkage, stator resistance and stator inductance, respectively. The electromagnetic torque of PMSM is expressed as

$$T_{ei}=\frac{3}{2}p\left[\psi_{fi}i_{qi}+(L_d-L_q)i_{di}i_{qi}\right]. \tag{2}$$

For surface permanent magnet synchronous motor (SPMSM), $L_d=L_q$, so the electromagnetic torque equation of the ith SPMSM can be expressed as

$$T_{ei}=\frac{3}{2}p_i\psi_{fi}i_{qi}. \tag{3}$$

The motion equation of PMSM is expressed as

$$J_i\frac{\mathrm{d}\omega_{mi}}{\mathrm{d}t}=T_{ei}-T_{Li}, \tag{4}$$

where T_{Li} represents the load torque, T_{ei} represents the electromagnetic torque, and J_i respresents the rotor inertia.

1.2 Unified prediction model of dual-motor

Based on the cross coupling control structure, this study improves the speed synchronization control system of dual-PMSM. The structure diagram of the synchronous speed control system based on the unified prediction model of dual-motor is shown in Fig. 1.

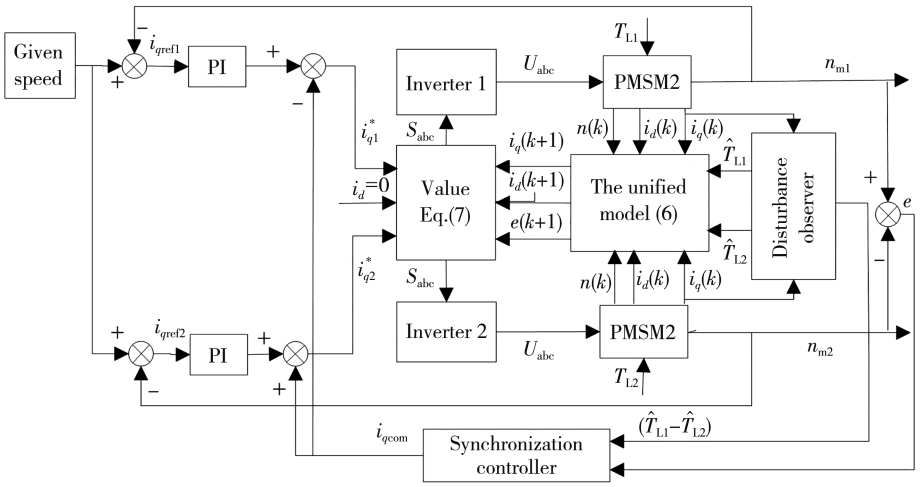

Fig. 1 Structure diagram of synchronous speed control system based on dual-motor unified prediction model

According to Eq. (4), the change rate of speed synchronization error can be obtained as

$$\frac{\mathrm{d}e}{\mathrm{d}t}=\frac{\mathrm{d}}{\mathrm{d}t}(\omega_{m1}-\omega_{m2})=\frac{1}{J_1}(T_{e1}-T_{L1}-B_1\omega_{m1})-\frac{1}{J_2}(T_{e2}-T_{L2}-B_2\omega_{m2}). \tag{5}$$

When establishing the unified prediction mathematical model, the motor and inverter are regarded as a whole, and the change rate of speed synchronization error is regarded as a state variable of the system. The unified prediction model of dual-PMSM can be obtained as

$$I(k+1)=G(k)I(k)+FU(k)+KD(k), \tag{6}$$

where

$$I(k)=[i_{d1}(k)\ \ i_{q1}(k)\ \ i_{d2}(k)\ \ i_{q2}(k)\ \ \omega_1(k)\ \ \omega_2(k)\ \ e(k)]^{\mathrm{T}},$$

$$U(k)=[u_{d1}(k)\ \ u_{q1}(k)\ \ u_{d2}(k)\ \ u_{q2}(k)\ \ \hat{T}_{L1}\ \ \hat{T}_{L2}]^{\mathrm{T}},\quad D=[D_1(k)\ \ D_2(k)]^{\mathrm{T}};$$

$$G(k)=\begin{bmatrix} A_1 & B_1(k) & 0 & 0 & 0 & 0 & 0\\ -B_1(k) & A_1 & 0 & 0 & 0 & 0 & 0\\ 0 & 0 & A_2 & B_2(k) & 0 & 0 & 0\\ 0 & 0 & -B_2(k) & A_2 & 0 & 0 & 0\\ 0 & C_1 & 0 & 0 & (1-B_1)T & 0 & 0\\ 0 & 0 & 0 & C_2 & 0 & (1-B_2)T & 0\\ 0 & C_1 & 0 & -C_2 & -B_1T & B_2T & T \end{bmatrix},$$

$$F=\begin{bmatrix} F_1 & 0 & 0 & 0 & 0 & 0\\ 0 & F_1 & 0 & 0 & 0 & 0\\ 0 & 0 & F_2 & 0 & 0 & 0\\ 0 & 0 & 0 & F_2 & 0 & 0\\ 0 & 0 & 0 & 0 & -T & 0\\ 0 & 0 & 0 & 0 & 0 & -T\\ 0 & 0 & 0 & 0 & -T & T \end{bmatrix},\quad K=\begin{bmatrix} 0 & 0\\ -1 & 0\\ 0 & 0\\ 0 & -1\\ 0 & 0\\ 0 & 0\\ 0 & 0 \end{bmatrix},$$

where T is the control period of the system; $\hat{T}_{L1}$ and $\hat{T}_{L2}$ are load observation values of motor 1 and mortor 2, respectively; $A_i=1-TR_i/L_i$, $B_i(k)=T\omega_{mi}(k)$, $C_i=\frac{3}{2}Tn_{pi}\psi_{fi}$, and $D_i(k)=T\omega_i(k)/(L_iF_i)=T/L_i(i=1,2)$.

1.3 Construction of value function

Compared with the traditional dual motor speed synchronous control system, this study adopts the piecewise value function, and the control principle is shown as

$$g=\begin{cases}g', & e<e_{\lim},\\ g'', & e\geqslant e_{\lim}\text{ for motor 1},\\ g''', & e\geqslant e_{\lim}\text{ for motor 2},\end{cases}\tag{7}$$

where e_{lim1} is the threshold, when $e\geqslant e_{lim1}$, the two motors are controlled by g'' and g''', respectively. When the motor is disturbed, the tracking error is adjusted first to make the system speed quickly track the given speed. When $e<e_{lim1}$, g' is adopeed, and the two motors are controlled by the same value function to achieve synchronization performance. g', g'' and g''' are expressed as

$$g'=g_1+g_2+\lambda g_3,\tag{8}$$

$$g''=|i_{d1}^*-i_{d1}(k+1)|+|i_{q1}^*-i_{q1}(k+1)|+\mu_1[\omega^*-\omega_1(k+1)],\tag{9}$$

$$g'''=|i_{d2}^*-i_{d2}(k+1)|+|i_{q2}^*-i_{q2}(k+1)|+\mu_2[\omega^*-\omega_2(k+1)],\tag{10}$$

where $g_1=|i_{d1}^*-i_{d1}(k+1)|+|i_{q1}^*-i_{q1}(k+1)|$, $g_2=|i_{q1}^*-i_{q1}(k+1)|+|i_{q2}^*-i_{q2}(k+1)|$, $g_3=|\omega_1(k+1)-\omega_2(k+1)|$.

In order to obtain better control performance, a value function includes the constraints of d-q axis current, speed tracking error and synchronization error. The weight coefficient is used to weigh the constraints. The synchronization error and tracking error are mutually restricted during adjustment, and the weight coefficient is difficult to set. In this study, the piecewise value function is established. The system uses different value functions in different operation stages to adjust the synchronization error and tracking error, respectively, so as to achieve better control effect.

2 Compound synchronization controller

2.1 Design of synchronization controller

In order to improve the dynamic performance and synchronization accuracy of the dual-motor control system, a PI + FOSMC compound synchronization controller is designed to compensate the current. The PI control keeps the system at a high steady-state accuracy, and the FOSMC control can enhance the anti-disturbance ability of the system. The structure of compound synchronization control system is shown in Fig. 2.

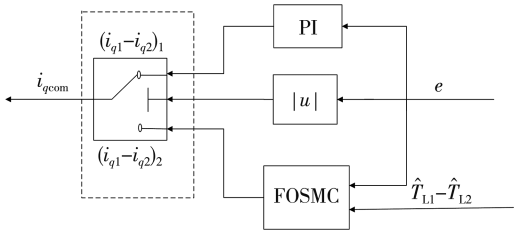

Fig. 2 Compound synchronous controller

The controller switches according to threshold e_{lim2}. When the motor is disturbed, the synchronization error is large, that is, $e\geqslant e_{lim2}$, in this case, the PI control is used, and the speed of the two motors quickly returns to synchronization; otherwise, the FOSMC control is switched.

2.1.1 Design of FOSMC

1) Design of sliding surface

The fractional integral sliding surface is designed as

$$s=e(t)+c_1D^{-\mu}e(t),\tag{11}$$

where $e(t)=\omega_{m1}-\omega_{m2}$, ω_{m1} is the speed of motor 1, and ω_{m2} is the speed of motor 1; c_1 is the fractional order integral constant; $0<\mu<1$, which is the order of the fractional order integral sliding surface.

In order to ensure the global robustness of the system, the integral sliding mode surface of fractional order is designed as

$$s=e(t)+c_1D^{-\mu}e(t)+h(t),\tag{12}$$

where $h(t)=h(0)e^{-\frac{t}{n}}$, and n determines the convergence rate of $h(t)$, with $n>0$.

Let $m=h(0)=-e(0)-c_1\times{}_0D_0^{-\mu}e(0)$, where ${}_0D_0^{-\mu}e(0)$ denotes the integral value at time t. We get $t=0$, $s=0$, which means that the system is on the sliding surface from the initial state and can be expressed as

$$s=e(t)+c_1D^{-\mu}e(t)+me^{-\frac{t}{n}}.\tag{13}$$

Then, we get the differential of Eq. (13) as

$$\dot{s}=\dot{e}(t)+c_1D^{1-\mu}e(t)-\frac{m}{n}\mathrm{e}^{-\frac{t}{n}}. \tag{14}$$

2) Design of reaching law

The constant velocity reaching law is adopted as

$$\dot{s}=-\varepsilon\,\mathrm{sgn}(s), \tag{15}$$

where ε is the sliding mode gain, with $\varepsilon>0$, and sgn(•) is the sign function.

According to Eqs. (4), (12) and (15), the output of FOSMC is

$$i_{q1}-i_{q2}=\frac{2J}{3p\psi_{\mathrm{f}}}\left[-\varepsilon\,\mathrm{sgn}(s)-c_1D^{1-\mu}e(t)+\frac{1}{J}(T_{\mathrm{L1}}-T_{\mathrm{L2}})\right]. \tag{16}$$

2.1.2 Stability analysis

To prove the stability of the FOSMC synchronization controller designed, we define the Lyapunov function as

$$V=\frac{1}{2}s^2. \tag{17}$$

According to Lyapunov stability theorem, the stability condition is $\dot{V}=s\dot{s}<0$.

Taking the derivative of Eq. (17) and substituting Eqs. (14)—(16) into it, we can get

$$\begin{aligned}\dot{V}=s\dot{s}&=s[D^{1-\mu}(D^{\mu}s)]=\\ &s\left[\dot{e}(t)+c_1D^{1-\mu}e(t)-\frac{m}{n}e(t)^{-\frac{t}{n}}\right]=\\ &s\left[\dot{\omega}_{\mathrm{m1}}-\dot{\omega}_{\mathrm{m2}}+c_1D^{1-\mu}e(t)-\frac{m}{n}e(t)^{-\frac{t}{n}}\right]=\\ &s\left[\frac{1}{J_1}\left(\frac{3}{2}p_n\psi_{\mathrm{f}}i_{q1}-T_{\mathrm{L1}}-B\omega_{\mathrm{m1}}\right)-\right.\\ &\frac{1}{J_2}\left(\frac{3}{2}p_n\psi_f i_{q2}-T_{\mathrm{L2}}-B\omega_{\mathrm{m2}}\right)+\\ &\left.c_1D^{1-\mu}e(t)-\frac{m}{n}e(t)^{-\frac{t}{n}}\right]=\\ &s[-\varepsilon\,\mathrm{sgn}(s)]=-\varepsilon\mid s\mid,\end{aligned} \tag{18}$$

where B is the self-damping coefficient.

It can be seen that when $\varepsilon>0$, the Lyapunov stability condition is satisfied. Therefore, the FOSMC synchronization controller designed is stable.

2.2 Design of disturbance observer

In practical applications, the load is variable and difficult to measure. Therefore, the sliding mode disturbance observer is designed to observe the load change of two motors, respectively, and the observed value is taken as the input of FOSMC to improve the ability of anti load disturbance. Taking the rotor mechanical angular velocity and the motor load torque as the state variables, combining Eqs. (3) and (4), the state equation is obtained as

$$\begin{cases}\dfrac{\mathrm{d}\omega_{\mathrm{m}}}{\mathrm{d}t}=\dfrac{1}{J}\left(\dfrac{3}{2}p\psi_{\mathrm{f}}i_q-T_{\mathrm{L}}-B\omega_{\mathrm{m}}\right),\\ \dfrac{\mathrm{d}T_{\mathrm{L}}}{\mathrm{d}t}=0.\end{cases} \tag{19}$$

The observation equations of rotor mechanical angular velocity and load torque are constructed as

$$\begin{cases}\dfrac{\mathrm{d}\hat{\omega}_{\mathrm{m}}}{\mathrm{d}t}=\dfrac{1}{J}\left(\dfrac{3}{2}p\psi_{\mathrm{f}}i_q-\hat{T}_{\mathrm{L}}-B\omega_{\mathrm{m}}\right)+U,\\ \dfrac{\mathrm{d}\hat{T}_{\mathrm{L}}}{\mathrm{d}t}=gU,\end{cases} \tag{20}$$

where $U=ksat(s)$, $sat(s)$ is a saturation function, g is the feedback gain, and k is the sliding mode gain.

Thus, the observation error equation is obtained as

$$\begin{cases}\dot{e}_1=-\dfrac{1}{Je_2}-\dfrac{B}{J}e_1+U,\\ \dot{e}_2=gU,\end{cases} \tag{21}$$

where $e_1=\hat{\omega}-\omega$ is the observation error of speed, and $e_2=\hat{T}_{\mathrm{L}}-T_{\mathrm{L}}$ is the observation error of load torque.

The sliding surface is

$$s=\hat{\omega}-\omega_{\mathrm{m}}. \tag{22}$$

The structure block diagram of sliding mode load observer is shown in Fig. 3.

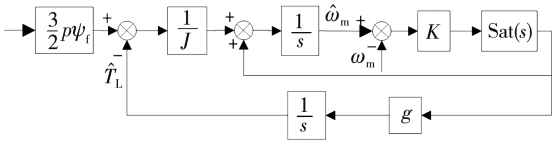

Fig. 3 Structure diagram of disturbance observer

When the observed load is brought into Eq. (17), the output of FOSMC can be obtained as

$$i_{q1}-i_{q2}=\frac{2J}{3p\psi_{\mathrm{f}}}\left[-\varepsilon\,\mathrm{sgn}(s)-c_1D^{1-\mu}e(t)+\frac{1}{J}(\hat{T}_{\mathrm{L1}}-\hat{T}_{\mathrm{L2}})\right]. \tag{23}$$

3 Simulation

In order to verify the effectiveness of the control strategy, Matlab/Simulink is used as simulation platform. The parameters of the two motors are shown in Table 1. System 1 is a traditional dual-motor speed synchronous control system, PI controller is used as the synchronous controller, and the controller parameters are $k_P=50$ and $k_I=8.5$. System 2 is the control system designed designed, and the parameters of compound controller are shown in Table 2.

Table 1 Parameters of traditional PMSM

Parameter	Value
DC bus voltage U_{dc}/V	300
Rated power P_N/kW	1.1
Rated torque T_N/(N·m)	3
Number of pole pairs p	2
Stator resistance R_s/Ω	2.875
Rotor magnetic flux Ψ_f/kHz	0.175
Stator inductance L_s/H	0.008 5
inertia coefficient J/(kg·m^{-2})	0.000 8

Table 2 Parameters of compound speed synchronization controller

Parameter	Value
k_p	50
k_I	8.5
Sliding mode gain ε	2 000
Fractional order μ	0.5
Fractional integral constant c_1	2 000
n	20
e_{lim2}	0.01

3.1 Starting under unbalanced load

In order to verify the influence of load disturbance on synchronization error, the speed of two motors is given as 1 000 r/min, PMSM1 starts at a load torque of 2 N·m, and PMSM2 starts under a load of 3 N·m. The simulation curves of the two systems are shown in Figs. 4—7.

It can be seen from Figs. 4 and 5 that system 1 fluctuates between 980 r/min and 1 020 r/min before reaching the given speed, with speed overshoot of 1.95% (motor 1). Moreover, the synchronization error is large in the speed rising stage, and the maximum synchronization error is more than 100 r/min. Figs. 6 and 7 show that the speed overshoot of system 2 is less than 0.67% (motor 1), and no fluctuations. Therefore the system 2 is stable in operation and the maximum synchronization error is no more than 1 r/min, which achieves good synchronization.

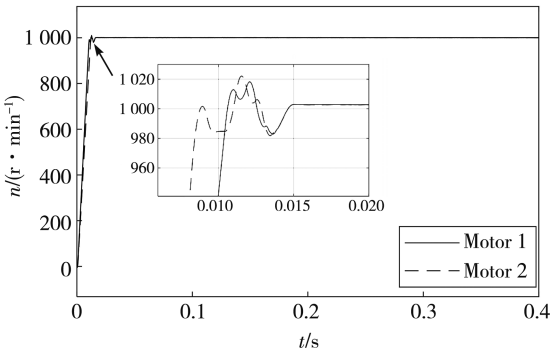

Fig. 4 Speed tracking curve of system 1 starting under unbalanced load

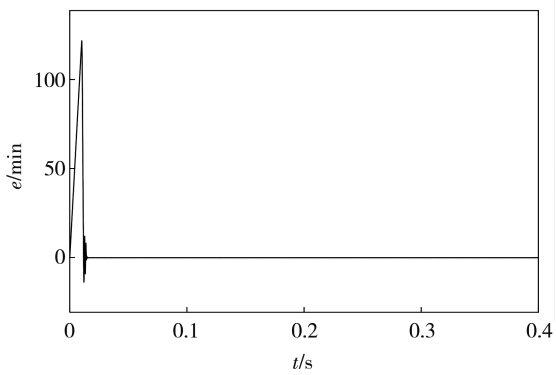

Fig. 5 Speed synchronization error curve of system 1 starting under unbalanced load

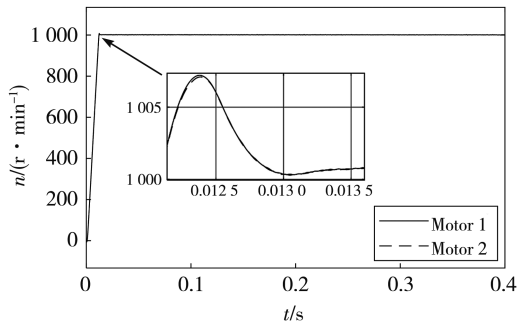

Fig. 6 Speed tracking curve of system 2 starting under unbalanced load

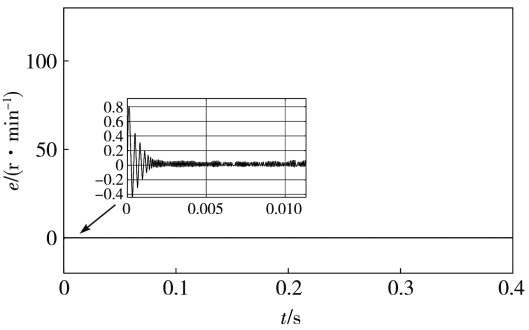

Fig. 7 Speed synchronization error curve of system 2 starting under unbalanced load

3.2 Variable speed operation

For speed variation in practical applications such as electric vehicles, the following simulation experiments are carried out for this phenomenon.

The system starts with no load, the speeds of two motors are given as 1 000 r/min, with a load torque of 2 N·m at 1.0 s applied to PMSM1, a load torque of 3 N·m at 3.0 s applied to PMSM2, and a sudden acceleration to 1 200 r/min at 0.2 s. The simulation curves are shown in Figs. 8—11.

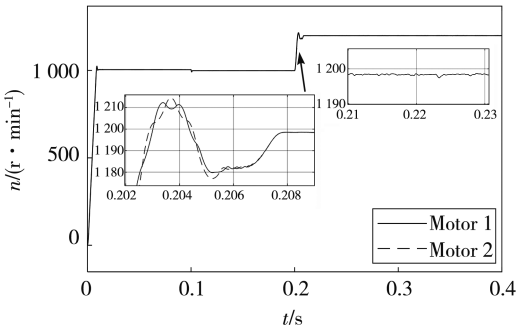

Fig. 8 Speed tracking curve of system 1 under variable speed operation

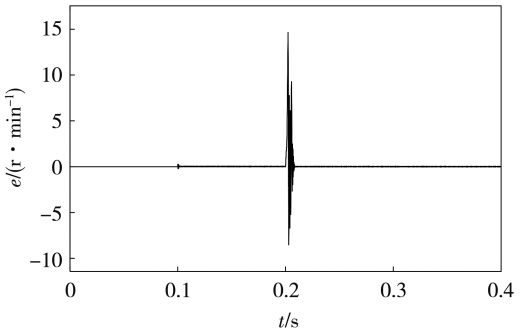

Fig. 9 Speed synchronization error curve of system 1 under variable speed operation

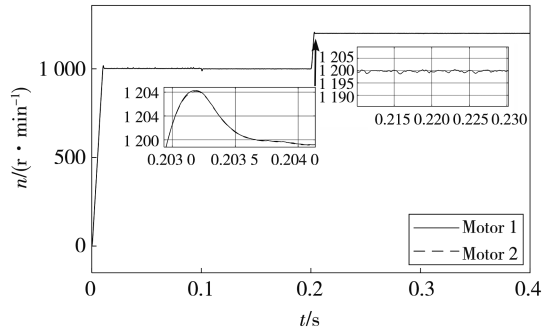

Fig. 10 Speed tracking curve of system 2 under variable speed operation

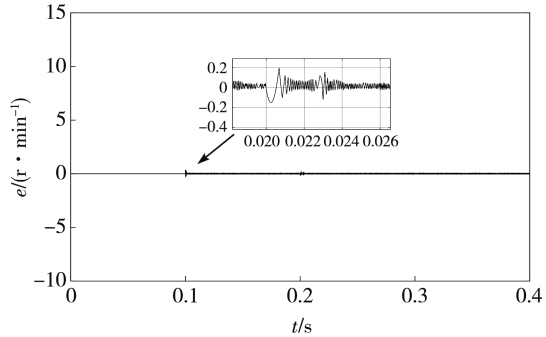

Fig. 11 Speed synchronization error curve of system 2 under variable speed operation

It can be seen from Figs. 8 and 10 that when the speed of system 2 increases from 1 000 r/min to 1 200 r/min, the speed of system 2 is stable and the speed of regulation is faster, while the speed of system 1 fluctuates greatly. When the system is running at 1 200 r/min, the tracking ability of system 2 is better, which basically remains at 1 200 r/min, while the speed of system 1 is 1 198 r/min. At the same time when the speed increases from 1 000 r/min to 1 200 r/min, the synchronization error of system 2 decreases obviously, and the maximum error does not exceed 1 r/min, while the maximum synchronization error of system 1 is 15 r/min.

3.3 Robustness verification of motor parameters

Since there exists difference in the parameters of the two motors, when the motor is running, the friction of the components or the heating of the system will cause the parameter changes. For example, the motor temperature will increase with the running time, and the resistance will increase with the temperature.

Taking the resistance of two motors as the variable parameter, the simulation experiment is carried out. When the system runs under noload, the resistance of motor 1 is set to be 2.675 Ω, and the resistance of motor 2 is set to be 2.875 Ω, which increases with time during operation, the simulation results are shown in Figs. 12—13.

The simulation results show that when the system has parameter disturbance, the synchronization error of system 1 is relatively large in the speed rising stage, which is more than 1 r/min, while system 2 basically has smaller synchronization error, which means that it has strong ability to resist parameter disturbance.

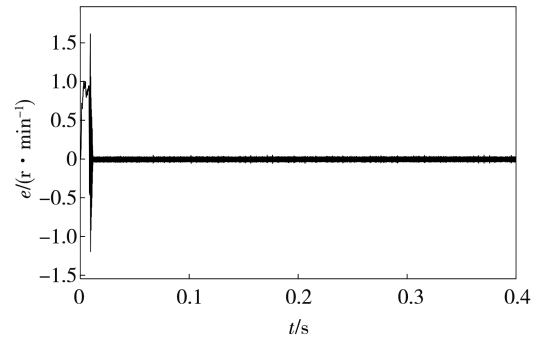

Fig. 12 Speed synchronization error curve of system 1 with parameter disturbance

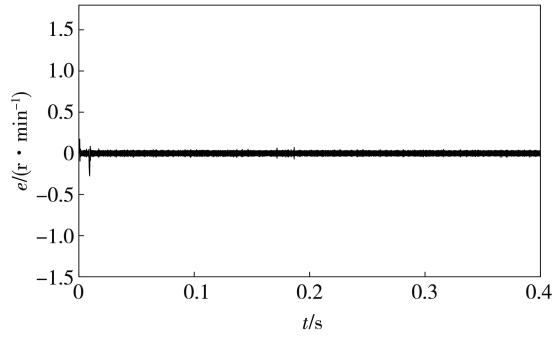

Fig. 13 Speed synchronization error curve of system 2 with parameter disturbance

4 Conclusions

Aiming at the speed synchronization problem of dual-motor control system, combined with cross-coupling control, a speed synchronization control system based on dual-motor unified prediction model is designed. The simulation results show that the control system designed has better control performance under various operating conditions. Its main characteristics are as follows:

1) The dual-motor unified prediction model provides the possibility to expand it to multi-motor synchronous control. The piecewise value function is introduced, which can more accurately adjust the speed tracking error and synchronization error.

2) The PI+FOSMC synchronization controller is established. The results show that the overshoot of motor speed in system 2 is smaller, the adjusting time is faster and the speed is more stable. When starting with load, it has strong anti-interference ability and robustness to the change of resistance parameters. The speed synchronization accuracy of two motor is improved.

References

[1] DING H C, LAI R, YANG X D, et al. A new sliding mode control for PMSM systems of a twoaxis turntable// IEEE International Conference on Mechatronic Sciences, Electric Engineering and Computer, Dec. 20-22, 2013, Shenyang, China. New York: IEEE, 2013: 135-138.

[2] XIA C L, LI L , GU X, et al. Speed synchronization control of dual-PMSM system. Transactions of China Electrotechnical Society, 2017, 32(23): 1-8.

[3] LI D L, MIAO Z C, WANG Z H, et al. Synchronous flux weakening control strategy of multi-motor system based on model prediction. Motor and Control Applications, 2019, 46(11): 7-12.

[4] YANG C Y, MENG F Y, XU Y M, et al. Coordinated control methods for multi-motor drive systems of large inertia load: a survey. Motor and Control Applications, 2019, 46(3): 1-7.

[5] SHI T N, LIU H, GENG Q, et al. Improved relative couplingcontrol structure for multi-motor speed synchronous driving system. IET Electric Power Applications, 2016, 10(6): 451-457.

[6] ZHU C, TU Q, JIANG C, et al. A cross coupling control strategy for dual-motor speed synchronous system based on second order global fast terminal sliding mode control. IEEE Access, 2020, 8: 217967-217976.

[7] WEI Y C, XIA C L, LIU T, et al. Finite control set model predictive control for dual-motor torque synchronous sysetm. Journal of Electrotechnical Society, 2016, 31(19): 115-122.

[8] VILLARROEL F, ESPINOZA J R, ROJAS C A, et al. Multi-objective switching state selector for finite-states model predictive control based on fuzzy decision making in a matrix converter. IEEE Transactions on Industrial Electronics, 2013, 60(2): 589-599.

[9] LV S S, LIN H. Model predictive direct torque control for PMSM with duty cycle optimization//IEEE International Conference on Instrumentation and Measurement, Computer, Communication and Control, Sept. 18-20, 2015, Qinhuangdao, China. New York: IEEE, 2015: 866-871.

[10] ZHENG Z D, WANG K, LI Y D, et al. Current controller for AC motors using model predictive control. Journal of Electrotechnical Society, 2013, 28(11): 118-123.

[11] TU W C, LUO G Z, LIU W G. Finite-control-set model predictive current control for permanent magnet synchronous motor based on dynamic cost function using fuzzy method. Journal of Electrotechnical Society, 2017, 32(16): 89-97.

[12] WANG Z Q, ZHANG X Y. Non-cascaded predictive speed synchronous control of dual permanent magnet synchronous motor system. Micromotor, 2020, 53(6): 78-86.

[13] SHI T N, YANG Y Y, ZHOU Z Q, et al. FCS-MPC for dual-motor torque synchronization system based on quadratic form cost function. Journal of China Electromechanical Engineering, 2019, 39(15): 4531-4541.

[14] ZHU R, WU D, CHEN J F, et al. A review of research on motor system model predictive control. Motor and Control Applications, 2019, 46(8): 1-10.

[15] XIA C Y, SADIQ U R, LIU Y. Analysis and design of current regulator stability during high-speed operation of permanent magnetic synchronous motor. Journal of China Electromechanical Engineering, 2020, 40(S1): 303-312.

[16] LI S H, ZHOU M M, YU X H. Design and implementation of terminal sliding mode control method for PMSM speed regulation systems. IEEE Transactions on Industrial Informatics, 2013, 9(4): 1879-1891.

[17] HAN T L, MIAO Z C, YU X F, et al. Fractional sliding mode control of mine motor based on load observation. Control Engineering, 2019, 26(11): 2052-2060.

[18] MIAO Z C, HAN T L, DANG J W, et al. Dynamic

fractional sliding mode control of induction motor with load observation. Acta Energiae Solaris Sinica, 2019, 40(2): 404-411.

[19] MIAO Z C, DANG J W, JU M, et al. Induction motor sensor-less vector control based on fractional order integral sliding mode observer. Electric Machines and Control, 2018, 22(5): 84-93.

[20] GAO Y, BU F, YANG Z, et al. Improved speed synchronization control algorithm based on cross coupling for dual servo motors control//International Conference on Electrical Machines and Systems, Oct. 7-10, 2018, Jeju Island, Korea. New York: IEEE, 2018: 2777-2780.

[21] LIN S Y, CAI Y Z, YANG B, et al. Electrical line-shafting control for motor speed synchronisation using sliding mode controller and disturbance observer. IET Control Theory & Applications, 2017, 11(2): 205-212.

双 PMSM 统一模型预测系统的转速同步控制

缪仲翠[1,2], 何阳阳[1], 李海源[1], 王运坤[1]

(1. 兰州交通大学 自动化与电机工程学院, 甘肃 兰州 730070;
2. 兰州交通大学 光电技术与智能控制教育部重点实验室, 甘肃 兰州 730070)

摘　要: 双电机控制系统中, 负载扰动、参数变化以及加减速运行等因素都会导致系统不稳定, 同步误差增大。针对以上问题, 设计了一种基于双电机统一预测模型的转速同步控制系统。首先, 在传统的双电机交叉耦合控制结构的基础上, 建立双电机统一模型, 并构造分段价值函数以更精确地调节跟踪误差和同步误差。其次, 为提高系统的动态性能和鲁棒性, 设计了比例积分和分数阶滑模复合同步控制器(Proportional integral+fractional order sliding mode control, PI+FOSMC)。最后, 在两台永磁同步电机(Permanent magnet synchronous motor, PMSM)上进行了仿真。结果表明, 双电机统一模型预测系统具有较强的动态性能和鲁棒性, 可提高系统同步精度。

关键词: 永磁同步电机; 双电机控制; 交叉耦合控制; 统一预测模型; 转速同步控制器; 同步精度

引用格式: MIAO Zhongcui, HE Yangyang, LI Haiyuan, et al. Dual-PMSM speed synchronization control based on unified prediction model. Journal of Measurement Science and Instrumentation, 2023, 14(3): 315-323. DOI: 10.3969/j.issn.1674-8042.2023.03.008